Nanoscale

COMMUNICATION

View Article Online
View Journal

Cite this: DOI: 10.1039/d3nr04086k

Received 14th August 2023,
Accepted 6th November 2023

DOI: 10.1039/d3nr04086k

rsc.li/nanoscale

Heteromeric guanosine (G)-quadruplex derived antenna modules with directional energy transfer†

Mohammad Amin Zarandi, [a] Pravin Pathak, [a] Noah Beltrami,[a] Jada N. Walker, [b] Fengqi Zhang,[a] Jennifer S. Brodbelt, [b] Russell Schmehl [a] and Janarthanan Jayawickramarajah *[a]

A heteromeric guanosine (G)-quadruplex centered self-assembly approach is developed to prepare compact light-harvesting antenna modules featuring multiple donor dyes and a single toehold region. Due to the mix-and-match nature of our approach, the number and placement of donor dyes can be readily fine-tuned *via* quadruplex assembly. Moreover, hybridization of the toehold with an acceptor containing sequence results in directional energy transfer ensembles with effective absorption coefficients in the 10^5 M^{-1} cm^{-1} range. These compact antennas exhibit system efficiencies that are comparable to much larger and elaborate DNA architectures containing numerous DNA strands.

Inspired by natural photosynthesis, artificial light harvesting antenna systems composed of judiciously arrayed donor and acceptor chromophores have been constructed for potential applications in optoelectronics, photovoltaic solar cells, sensors and light-based storage and encryption devices.[1–11] These systems generally involve the use of synthetic templates (polymers, dendrimers, metal–organic frameworks) or biological scaffolds (such as protein-based viral capsids) to position dyes in a well-defined, nanometer regime, for light absorption and funneling.[12–24] Among the various scaffolding technologies, DNA is arguably unrivaled due to the diversity and programmability of 3D structures that can be assembled using DNA, with precision placement of dyes.[25–31] Further advantages of DNA include its compatibility with biological systems and facile post-synthesis modification.

The majority of the DNA-based photonic ensembles prepared thus far have focused on either stand-alone DNA double helices, or elegant structures derived from DNA double helices, such as multiway junctions, DNA tile structures, and DNA origami.[32–45] These higher-order architectures enable the positioning of multiple dyes in a well-defined manner. However, their scaffolding economy, in terms of length and number of DNA sequences used is typically large. Our group is interested in developing compact antenna systems with high dye density whilst utilizing a minimal amount of DNA.[46,47] In this regard, tetramolecular parallel guanosine (G)-quadruplexes (Gq_{hom}) composed of the self-assembly of homomeric (*i.e.*, identical) oligodeoxynucleotide (ODN) sequences are a promising scaffold for building nanophotonic devices since multiple chromophores can be easily arrayed with well-defined spatial arrangement using the assembly of just one short ODN. Further strengths of (G)-quadruplexes are their thermal stability and nuclease resistance.[48–51]

A few fluor-containing Gq_{hom} have been investigated.[52–54] For instance, Zhu and coworkers used Gq_{hom} to position dyes capable of aggregation induced emission (AIE), resulting in fine control of fluorescence (Fig. 1A, left).[55] Taking an opposite approach, Gq_{hom} have been appended to porphyrin chromophores that are precluded from aggregating (*via* host encapsulation) resulting in significantly increased absorption and emission capacity (Fig. 1A, right).[46,47,56] Although, these examples illustrate the potential of using (G)-quadruplexes to assemble dye units for photonic applications, due to the symmetric nature of Gq_{hom}, it remains a challenge to construct directional energy funneling systems. Margulies *et al.* devised an innovative method for creating an antiparallel heteromeric G-quadruplex scaffold tethered to different fluorophores for user-authorization applications.[57] However, their system uses 4 long sequences (34 nucleotides) and must first form a complex four-way junction which enables G-quadruplex formation upon addition of sodium ions.

Herein, we report the first example of heteromeric parallel tetramolecular (G)-quadruplex (Gq_{het}) based antenna modules bearing a single overhang. Further, these modules are capable of directional energy migration from multiple donor chromophores to a single energy acceptor (Fig. 1B). In particular, 3 distinct Gq_{het} species positioned with fluorescein dyes at the 5′ and/or 3′ ends of the quadruplex region and featuring a single overhanging toehold region were constructed (**GqI–GqIII**).

[a]*Department of Chemistry, Tulane University, New Orleans, LA, 70118, USA. E-mail: jananj@tulane.edu*
[b]*Department of Chemistry, The University of Texas at Austin, Austin, TX 78712, USA*
† Electronic supplementary information (ESI) available. See DOI: https://doi.org/10.1039/d3nr04086k

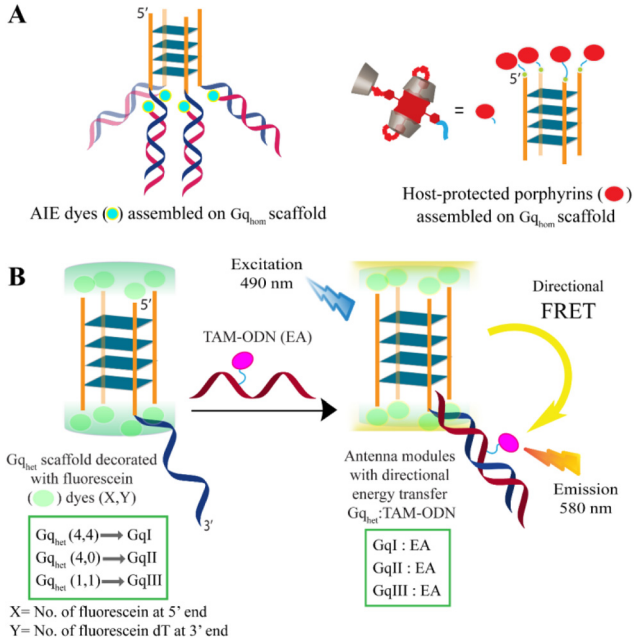

Fig. 1 (A) Previous examples of homomeric (G)-quadruplex scaffolds with specifically positioned dyes with enhanced fluorescence properties. (B) Self-assembled heteromeric (G)-quadruplex antenna modules introduced in this work, wherein the number and position of energy donors can be modulated, and directional energy migration to an acceptor dye can be achieved.

Subsequently, directional energy funneling ensembles (**GqI : EA–GqIII : EA**) were prepared by straight-forward hybridization with an ODN containing a TAMRA acceptor (**EA**) that is complementary to the toehold region of **GqI–GqIII**. Importantly, our mix-and-match assembly strategy is versatile as it enables the construction of discrete light-harvesting ensembles where the donor ratio and their relative positioning can be readily dialed-in.

It is well known that short ODNs consisting of four or five consecutive guanines can form Gq$_{hom}$ in the presence of monovalent cations.[48,58] We reasoned that if two different ODNs that have an identical track of 5 Gs (but where one ODN also contains a single-stranded overhang) were self-assembled, a statistical mixture would form consisting of 5 discernible (G)-quadruplexes (2 Gq$_{hom}$ and 3 Gq$_{het}$).[47] Since (G)-quadruplexes with 5 rungs of Gs are stable,[48] non-denaturing polyacrylamide gel-electrophoresis (PAGE) could then be used to isolate the required Gq$_{het}$ species decorated with only 1 single-stranded tail. As shown in Fig. 2A, to investigate the feasibility of this strategy, we first exposed ODNs **1** and **2** (each containing two fluorescein dyes) to quadruplex forming conditions by annealing an equimolar mixture (50 μM) of the ODNs in K^+ buffer (100 mM potassium phosphate buffer, pH 7.3) at 95 °C for 10 minutes, followed by slow cooling to room temperature and incubation at 4 °C for 72 hours. ODN **1** contains a domain that includes 5 Gs and a region with a 16-mer tail (5′-FAM-TGGGGGAT^{FAM}AGCTGAGGTCACGTTA-3′) while ODN **2** (5′-FAM-TGGGGGAT^{FAM}-3′) lacks the tail sequence.

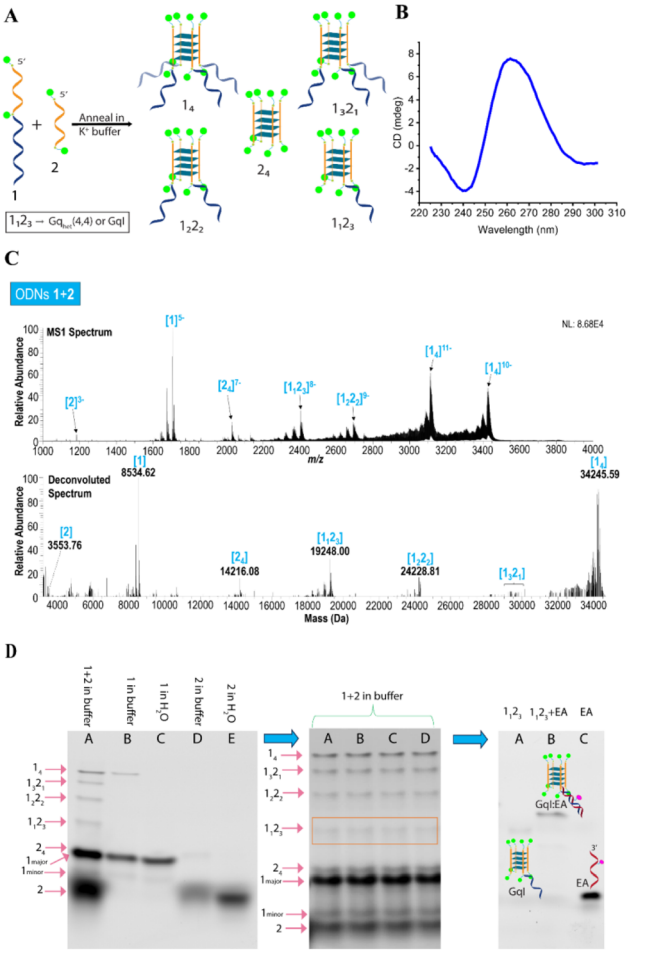

Fig. 2 (A) Schematic illustrating the various (G)-quadruplex species that are formed when ODNs **1** and **2** are self-assembled. (B) CD spectrum of self-assembled ODNs **1** and **2** (20 μM). (C) ESI-MS analysis of annealed ODNs **1** + **2**. (Upper) MS1 and (lower) deconvoluted mass spectrum of ODNs **1** + **2** in 150 mM ammonium acetate. (D) PAGE Studies: left. Lane A; self-assembly of ODNs **1** and **2** (50 μM) in K^+ buffer resulting in single stranded ODNs as well as Gq$_{hom}$ and Gq$_{het}$ species. Lane B; ODN **1** in K^+ buffer, lane C; ODN **1** in ultrapure water. Lane D; ODN **2** in K^+ buffer, and lane E; ODN **2** in ultrapure water. Note the concentrations loaded on lane A (50 μM per ODN) is 10× more than for the control lanes. Middle: **GqI** isolation and extraction. All lanes were loaded with self-assembled solution of ODNs **1** and **2** (50 μM). The orange box shows the band corresponding to **GqI**. Right: analytical PAGE (lane A) conducted on the retrieved **GqI** (**1$_1$2$_3$**) showing its integrity and migration. Also shown are **GqI** (**1$_1$2$_3$**) + **EA** (lane B), and **EA** only (lane C). For these studies, the quadruplex assembly buffer was 100 mM potassium phosphate buffer (53 mM K_2HPO_4 and 47 mM KH_2PO_4, pH 7.3). The running buffer was 1× TBE buffer containing 33 mM KCl.

To determine whether the assembly of ODNs **1** and **2** form parallel quadruplexes (mixture of Gq$_{hom}$ and Gq$_{het}$) circular dichroism (CD) spectroscopy was first conducted (Fig. 2B). The CD spectrum displays two characteristic peaks (a minimum at 240 nm and a maximum at 262 nm) consistent with the formation of parallel (G)-quadruplexes.[59]

Since electrospray ionization mass spectrometry (ESI-MS) can be used to examine G-quadruplex structures,[60] we next

analyzed the annealed solution of ODNs **1** and **2** by ESI-MS to confirm the stoichiometry of strands **1** and **2** within the resulting Gq_{hom} and Gq_{het} assemblies (Fig. 2C). Amongst the two Gq_{hom} species (*i.e.*, $\mathbf{1_4}$ and $\mathbf{2_4}$), the Gq_{hom} formed by **1** was more abundant compared to the Gq_{hom} formed by **2**. Moreover, ion peaks corresponding to the Gq_{het} assemblies $\mathbf{1_12_3}$, $\mathbf{1_22_2}$, and $\mathbf{1_32_1}$, in addition to single-stranded **1** and **2**, were also detected by ESI-MS. Subsequently, the ESI spectrum was decharged and deisotoped, yielding a deconvoluted mass spectrum with the mass and relative abundance of each species. $\mathbf{1_4}$ (34.2 kDa) was the most abundant of all the quadruplex species, and $\mathbf{1_12_3}$ (19.2 kDa) was most abundant amongst all Gq_{het} assemblies. The ESI results affirm that the annealed solutions of ODNs **1** and **2** can form a variety of G-quadruplex species with the expected combinations of strands **1** and **2**.

Next, the quadruplex assemblies were interrogated *via* non-denaturing PAGE to identify the specific Gq_{het} species. As can be seen from Fig. 2D, left (lane A) there is a fast-moving band that corresponds to the short single-strand **2** (compare with control lane E where **2** is not annealed in K^+ containing buffer). This is followed by two bands, that we assign to major and minor conformations of single stranded ODN **1** (*cf.* lane C, where **1** is not annealed in buffer). The major conformation of single strand **1** overlaps with Gq_{hom} of strand **2** (*cf.* lane D, where only **2** is annealed in buffer). The Gq_{hom} of strand **1** is observed to be the slowest migrating species (see control lane B, where **1** is annealed in buffer). In lane A, between the two Gq_{hom} species are 3 unique bands ascribed to Gq_{het} $\mathbf{1_12_3}$, $\mathbf{1_22_2}$, and $\mathbf{1_32_1}$. The self-assembly followed by PAGE experiments were repeated multiple times and the requisite Gq_{het} $\mathbf{1_12_3}$ band was cut, pooled, and extracted from the gel (by incubating in K^+ buffer at 4 °C for 48 hours; see Fig. 2D, middle). Shown in Fig. 2D, right (lane A), is the isolated Gq_{het} $\mathbf{1_12_3}$ that was rerun on PAGE, illustrating the integrity of the ensemble. In addition, the incubation of Gq_{het} $\mathbf{1_12_3}$ with TAMRA containing complementary strand **EA** (5′-TAACGT GACCT^{TAM}CAGCTAT-3′) (lane B) results in a discrete species attributed to **GqI : EA** (also observed with ESI-MS, see ESI Fig. S22†).

We next investigated the effectiveness of **GqI : EA** in serving as an antenna module *via* steady state fluorescence emission measurements (Fig. 1B). In this system, it was expected that the energy from the excited fluorescein donors will migrate to the TAMRA acceptor through homo- and ultimately hetero-FRET, resulting in emission from the acceptor moiety.[61] Specifically, **EA** was titrated into a solution containing **GqI** and the fluorescein donors were selectively excited (490 nm) until a maximum emission intensity from the TAMRA dye was reached. At this concentration of **EA**, it was assumed that a 1 : 1 complex (*i.e.*, **GqI : EA**) is formed (Fig. S5†).

As can be seen from inspection of Fig. 3A, selective excitation of the 8 fluorescein donors on **GqI** shows only donor emission (at 520 nm), with a high intensity (green profile). In contrast, when the fluorescein donors on the **GqI : EA** complex are excited (blue profile), the emission band at 520 nm is attenuated and a new longer wavelength band corresponding to

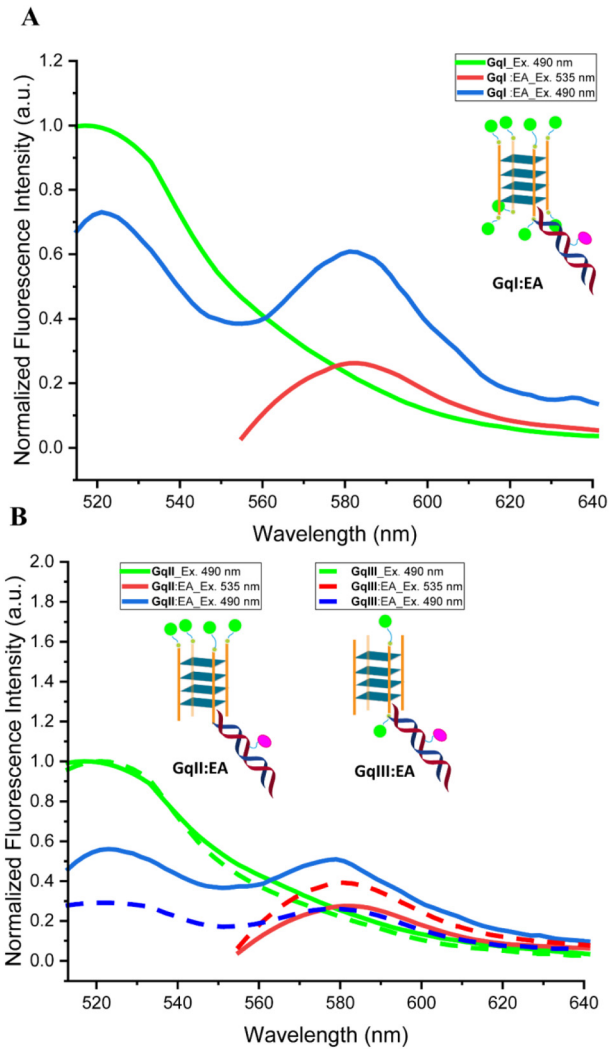

Fig. 3 Normalized steady-state fluorescence emission studies of (A) **GqI** and **GqI : EA**, and (B) **GqII–GqIII** and **GqII : EA–GqIII : EA**. Green curves: **GqI–GqIII**- ex. at 490 nm. Blue curves: **GqI : EA–GqIII : EA**- ex. at 490 nm. Red curves: **GqI : EA–GqIII : EA**- ex. at 535 nm.

the emission from the TAMRA acceptor is observed. From these quenching studies the overall energy transfer efficiency (E)[39] was determined to be 0.41 ± 0.12. Further, the antenna effect (AE; a measure of the light harvesting efficiency) for **GqI : EA** of 2.15 ± 0.10 was determined, by comparing the intensity of the TAMRA emission when fluorescein dyes are excited (blue profile) *versus* direct excitation of the TAMRA acceptor at 535 nm (red profile).[32] The effective absorption coefficient (ε_{eff}; which indicates the apparent absorption capacity of the acceptor at the donor excitation wavelength) for **GqI : EA** was calculated to be 1.16×10^5 M^{-1} cm^{-1} (see eqn (S10)†).[61]

In order to show the versatility of the Gq_{het} self-assembly approach, we also prepared antenna systems decorated with varying number of donors. This was achieved *via* similar heteromeric quadruplex assembly and gel-isolation studies using varying binary mixtures of ODNs **1**, **3**, **4**, and **5** (see Table S2,

and Fig. S17–S20†). The resultant Gq_{het} scaffolds containing a single overhang were then hybridized with **EA** and photophysical studies were conducted on the light harvesting ensembles (Fig. 3B).

Ensembles **GqII : EA** and **GqIII : EA** feature systems with four fluorescein donors (ODNs **3** + **4** + **EA** → **GqII : EA**) and two fluorescein donors (ODNs **1** + **5** + **EA** → **GqIII : EA**). Table 1 summarizes the photophysical properties of the antenna systems. Comparison of *E* indicates that ensemble with 2 donors (*i.e.*, **GqIII : EA**) has an increased overall energy transfer efficiency over ensembles with 4 or more donors (**GqI : EA** and **GqII : EA**). Detrimental donor–donor interactions can affect the overall energy transfer efficiency and hence Gq_{het} species with more donors are expected to show lower *E* values. Further, to investigate the donor–donor interactions in the absence of the acceptor, the fluorescence quantum yields (QY) of **GqI–GqIII** were estimated.[61] The QY results generally correlate with the observed energy transfer efficiencies. Although a larger number of donors can lead to more donor–donor interactions and more HOMO-FRET steps that can negatively impact *E*, in contrast, the AE values are enhanced for the antennas containing 4 and 8 donors. In particular, **GqI : EA** featuring 8 fluorescein dyes exhibits the most pronounced AE (2.15 ± 0.10). This compact antenna system shows system efficiencies that are comparable to much larger DNA architectures.[26,32,34] In particular, the overall ε_{eff} for **GqI : EA** is competitive with other higher-order and more elaborate DNA-based light harvesting systems with large numbers and types of donor dyes. For example, an elegant eight-way multi-junction based system containing 8 long DNA strands and 48 pyrene donor dyes with a central perylene acceptor exhibited an ε_{eff} of 1.7×10^5 M^{-1} cm^{-1}.[39]

In conclusion, we have disclosed a novel strategy to prepare light-harvesting antenna modules wherein the number and placement of donor dyes can be dialled-in using heteromeric DNA (G)-quadruplex self-assembly followed by gel-isolation. Moreover, these antenna systems feature a single overhang that can be used to hybridize with acceptor containing sequences to afford directional energy transfer ensembles with appreciable ε_{eff} values. Donor–donor interactions are an important factor and future efforts will focus on using dyes that have enhanced fluorescence when aggregating or using host-encapsulation strategies.[46,55] In addition, we note that our Gq_{het} strategy featuring a single-stranded toehold region could be of utility for the attachment of tetramolecular (G)-quadruplexes to other functional systems (*e.g.*, nanoparticles, surfaces, and higher-order DNA nanostructures) that contain complementary overhanging sequences.

Table 1 Photophysical properties of light harvesting ensembles **GqI : EA–GqIII : EA**. AE and *E* values are the mean of two separate experiments

Ensembles	AE	*E*	$\varepsilon_{eff} \times 10^5$ M^{-1} cm^{-1}	QY[a]
GqI : EA	2.15 ± 0.10	0.41 ± 0.12	1.16 ± 0.10	0.065
GqII : EA	1.77 ± 0.04	0.37 ± 0.10	0.96 ± 0.04	0.082
GqIII : EA	0.73 ± 0.08	0.68 ± 0.10	0.39 ± 0.08	0.150

[a] Estimated quantum yields for the parent quadruplexes **GqI–GqIII**.

Conflicts of interest

There are no conflicts to declare.

Acknowledgements

This work was supported by the NSF Grant CHE-2003879 to J. J. The characterization of DNA samples was performed on a Bruker Autoflex III matrix-assisted laser desorption time-of-flight mass spectrometer (MALDI-TOF MS) acquired *via* NSF CHE 0619770, or on a Bruker Daltonics Autoflex Speed MALDI-TOF/TOF acquired *via* NSF CHE 1625993. This research was also supported by the National Institutes of Health (R35GM139658, J. S. B.) and the Robert A. Welch Foundation [F-1155, J.S.B.].

References

1 B. Xie, Z. Chen, L. Ying, F. Huang and Y. Cao, *InfoMat*, 2020, **2**, 57–91.
2 Y. Zhang, Z. Wang and Y. C. Chen, *Prog. Quantum Electron.*, 2021, **80**, 100361.
3 O. Kulyk, L. Rocard, L. Maggini and D. Bonifazi, *Chem. Soc. Rev.*, 2020, **49**, 8400–8424.
4 C. E. Rowland, J. B. Delehanty, C. L. Dwyer and I. L. Medintz, *Mater. Today*, 2017, **20**, 131–141.
5 B. Albinsson, J. K. Hannestad and K. Börjesson, *Coord. Chem. Rev.*, 2012, **256**, 2399–2413.
6 G. S. Schlau-Cohen, *Interface Focus*, 2015, **5**, 20140088.
7 G. J. Hedley, A. Ruseckas and I. D. W. Samuel, *Chem. Rev.*, 2017, **117**, 796–837.
8 X. M. Chen, X. Chen, X. F. Hou, S. Zhang, D. Chen and Q. Li, *Nanoscale Adv.*, 2022, **5**, 1830–1852.
9 L. Wu, C. Huang, B. P. Emery, A. C. Sedgwick, S. D. Bull, X. P. He, H. Tian, J. Yoon, J. L. Sessler and T. D. James, *Chem. Soc. Rev.*, 2020, **49**, 5110–5139.
10 M. F. Fouz, K. Mukumoto, S. Averick, O. Molinar, B. M. McCartney, K. Matyjaszewski, B. A. Armitage and S. R. Das, *ACS Cent. Sci.*, 2015, **1**, 431–438.
11 D. Perumal, J. Krishna, K. S. Harikrishnan, G. Raj, J. Kalathil, M. Saji, M. Kavyasree and R. Varghese, *Nanoscale*, 2023, **15**, 8972–8977.
12 C. M. Spillmann and I. L. Medintz, *J. Photochem. Photobiol., C*, 2015, **23**, 1–24.
13 C. W. Brown, A. Samanta, S. A. Díaz, S. Buckhout-White, S. A. Walper, E. R. Goldman and I. L. Medintz, *Adv. Opt. Mater.*, 2017, **5**, 1700181.
14 A. Wollny, G. Lavarda, I. Papadopoulos, I. López-Duarte, H. Gotfredsen, Y. Hou, R. R. Tykwinski, T. Torres and D. M. Guldi, *Adv. Opt. Mater.*, 2023, **11**, 2300500.

15 I. Oh, H. Lee, T. W. Kim, C. W. Kim, S. Jun, C. Kim, E. H. Choi, Y. M. Rhee, J. Kim, W. D. Jang and H. Ihee, *Adv. Sci.*, 2020, **7**, 2001623.
16 V. Almeida-Marrero, E. Van De Winckel, E. Anaya-Plaza, T. Torres and A. De La Escosura, *Chem. Soc. Rev.*, 2018, **47**, 7369–7400.
17 J. Joseph, L. M. O. Lourenço, J. P. C. Tomé, T. Torres and D. M. Guldi, *Nanoscale*, 2022, **14**, 13155–13165.
18 Y. Z. Ma, R. A. Miller, G. R. Fleming and M. B. Francis, *J. Phys. Chem. B*, 2008, **112**, 6887–6892.
19 A. P. Singh, N. Kumar and A. P. Singh, *Mater. Today: Proc.*, 2023, **81**, 758–760.
20 Z. Wang and C. Wang, *Adv. Mater.*, 2021, **33**, 2005819.
21 M. A. Oar, W. R. Dichtel, J. M. Serin, J. M. J. Fréchet, J. E. Rogers, J. E. Slagle, P. A. Fleitz, L. S. Tan, T. Y. Ohulchanskyy and P. N. Prasad, *Chem. Mater.*, 2006, **18**, 3682–3692.
22 Q. Song, S. Goia, J. Yang, S. C. L. Hall, M. Staniforth, V. G. Stavros and S. Perrier, *J. Am. Chem. Soc.*, 2021, **143**, 382–389.
23 A. Nandy and S. Mukherjee, *J. Phys. Chem. Lett.*, 2022, **13**, 6701–6710.
24 A. J. Bischoff, L. M. Hamerlynck, A. J. Li, T. D. Roberts, N. S. Ginsberg and M. B. Francis, *J. Am. Chem. Soc.*, 2023, **145**, 15827–15837.
25 S. Hirashima, H. Sugiyama and S. Park, *J. Phys. Chem. B*, 2020, **124**, 8794–8800.
26 X. Zhou, D. Satyabola, H. Liu, S. Jiang, X. Qi, L. Yu, S. Lin, Y. Liu, N. W. Woodbury and H. Yan, *Angew. Chem., Int. Ed.*, 2022, **61**, e202211200.
27 H. Bui, S. A. Díaz, J. Fontana, M. Chiriboga, R. Veneziano and I. L. Medintz, *Adv. Opt. Mater.*, 2019, **7**.
28 X. Tang, Y. Zhu, W. Guan and C. Lu, *Aggregate*, 2023, **4**, e348.
29 N. Bürki, E. Grossenbacher, A. Cannizzo, T. Feurer, S. M. Langenegger and R. Häner, *Org. Biomol. Chem.*, 2020, **18**, 6818–6822.
30 J. K. Hannestad, P. Sandin and B. Albinsson, *J. Am. Chem. Soc.*, 2008, **130**, 15889–15895.
31 X. Zhou, S. Mandal, S. Jiang, S. Lin, J. Yang, Y. Liu, D. G. Whitten, N. W. Woodbury and H. Yan, *Efficient Long-range, Directional Energy Transfer through DNA-Templated Dye Aggregates*.
32 L. Olejko and I. Bald, *RSC Adv.*, 2017, **7**, 23924–23934.
33 R. J. Mazuski, S. A. Díaz, R. E. Wood, L. T. Lloyd, W. P. Klein, W. P. Klein, D. Mathur, D. Mathur, J. S. Melinger, G. S. Engel and I. L. Medintz, *J. Phys. Chem. Lett.*, 2020, **11**, 4163–4172.
34 E. A. Hemmig, C. Creatore, B. Wünsch, L. Hecker, P. Mair, M. A. Parker, S. Emmott, P. Tinnefeld, U. F. Keyser and A. W. Chin, *Nano Lett.*, 2016, **16**, 2369–2374.
35 Y. Choi, L. Kotthoff, L. Olejko, U. Resch-Genger and I. Bald, *ACS Appl. Mater. Interfaces*, 2018, **10**, 23295–23302.
36 W. P. Klein, B. S. Rolczynski, S. M. Oliver, R. Zadegan, S. Buckhout-White, M. G. Ancona, P. D. Cunningham, J. S. Melinger, P. M. Vora, W. Kuang, I. L. Medintz and S. A. Díaz, *ACS Appl. Nano Mater.*, 2020, **3**, 3323–3336.
37 F. Nicoli, A. Barth, W. Bae, F. Neukirchinger, A. H. Crevenna, D. C. Lamb and T. Liedl, *ACS Nano*, 2017, **11**, 11264–11272.
38 F. Garo and R. Häner, *Angew. Chem., Int. Ed.*, 2012, **51**, 916–919.
39 H. Kashida, H. Azuma, R. Maruyama, Y. Araki, T. Wada and H. Asanuma, *Angew. Chem., Int. Ed.*, 2020, **59**, 11360–11363.
40 C. D. Bösch, E. Abay, S. M. Langenegger, M. Nazari, A. Cannizzo, T. Feurer and R. Häner, *Helv. Chim. Acta*, 2019, **102**, e1900148.
41 I. H. Stein, V. Schüller, P. Böhm, P. Tinnefeld and T. Liedl, *ChemPhysChem*, 2011, **12**, 689–695.
42 C. V. Kumar and M. R. Duff, *J. Am. Chem. Soc.*, 2009, **131**, 16024–16026.
43 Z. Zhao, Y. Han and Y. Liu, *Opt. Mater. Express*, 2022, **12**, 284.
44 J. K. Hannestad, S. R. Gerrard, T. Brown and B. Albinsson, *Small*, 2011, **7**, 3178–3185.
45 T. N. Nguyen, A. Brewer and E. Stulz, *Angew. Chem., Int. Ed.*, 2009, **48**, 1974–1977.
46 P. Pathak, W. Yao, K. D. Hook, R. Vik, F. R. Winnerdy, J. Q. Brown, B. C. Gibb, Z. F. Pursell, A. T. Phan and J. Jayawickramarajah, *J. Am. Chem. Soc.*, 2019, **141**, 12582–12591.
47 N. Zhang, X. Chu, M. Fathalla and J. Jayawickramarajah, *Langmuir*, 2013, **29**, 10796–10806.
48 C. Bardin and J. L. Leroy, *Nucleic Acids Res.*, 2008, **36**, 477–488.
49 A. N. Lane, J. B. Chaires, R. D. Gray and J. O. Trent, *Nucleic Acids Res.*, 2008, **36**, 5482–5515.
50 J. Casals, J. Viladoms, E. Pedroso and C. González, *J. Nucleic Acids*, 2010, 468017, DOI: **10.4061/2010/468017**.
51 J. Jana and K. Weisz, *ChemBioChem*, 2021, **22**, 2848–2856.
52 N. Sancho Oltra, W. R. Browne and G. Roelfes, *Chem. – Eur. J.*, 2013, **19**, 2457–2461.
53 J. Cai, D. M. Niedzwiedzki, H. A. Frank and A. D. Hamilton, *Chem. Commun.*, 2010, **46**, 544–546.
54 J. Cai, E. M. Shapiro and A. D. Hamilton, *Bioconjugate Chem.*, 2009, **20**, 205–208.
55 L. Zhu, J. Zhou, G. Xu, C. Li, P. Ling, B. Liu, H. Ju and J. Lei, *Chem. Sci.*, 2018, **9**, 2559–2566.
56 J. Jayawickramarajah, D. M. Tagore, L. K. Tsou and A. D. Hamilton, *Angew. Chem., Int. Ed.*, 2007, **46**, 7583–7586.
57 O. Lustgarten, R. Carmieli, L. Motiei and D. Margulies, *Angew. Chem.*, 2019, **131**, 190–194.
58 F. Rosu, V. Gabelica, H. Poncelet and E. De Pauw, *Nucleic Acids Res.*, 2010, **38**, 5217–5225.
59 B. Zhou, Y. Geng, C. Liu, H. Miao, Y. Ren, N. Xu, X. Shi, Y. You, T. Lee and G. Zhu, *Sci. Rep.*, 2018, **8**, 2366.
60 S. E. Pierce, J. Wang, J. Jayawickramarajah, A. D. Hamilton and J. S. Brodbelt, *Chem. – Eur. J.*, 2009, **15**, 11244–11255.
61 J. G. Woller, J. K. Hannestad and B. Albinsson, *J. Am. Chem. Soc.*, 2013, **135**, 2759–2768.